The Journal of Undergraduate Research

Volume 4 *Journal of Undergraduate Research, Volume 4: 2006*

Article 4

2006

# Dynamical Multi-body Gyroscopic Motion Simulation

Andy Ries
*South Dakota State University*

Johnathan Deppe
*South Dakota State University*

# Dynamical Multi-body Gyroscopic Motion Simulation

Authors: Andy Ries, Jonathan Deppe
Faculty Sponsor: Dr. Shanzhong (Shawn) Duan
Department: Mechanical Engineering Department

## ABSTRACT

In this paper, the motion of a three-degree-of-freedom gyroscope is analyzed in three different force scenarios. The equations of motion for the gyroscope are derived by hand as well as derived by the dynamical analysis software, Autolev™. These equations are compared with each other to show the consistency between the two methods and the time savings of using software applications for analyzing complex multi-body dynamical systems. The Autolev™ program drastically reduced the workload for determining the motion equations and the program even compiled Matlab™ code that was used to produce numerical values to show the respective motion of each gyroscope component. The results from the Autolev™ code represent the expected rotational motion as well as some much unexpected rocking in the outer and inner gimbals when the inner rotor spun slowly enough. The overall results show the benefits of using Kane's equation and Autolev™ software for computer simulation of dynamic behaviors of a three-degree-of-freedom gyroscope. The results provide the first-hand experience for undergraduate research in the area of computational multi-body dynamics. Keywords: gyroscope, Kane's equation, Autolev, Matlab.

## INTRODUCTION

A gyroscope is an instrument that maintains an initial angular reference direction by virtue of a rapidly spinning mass (rotor). A standard gyroscope is spherical and only about three inches in diameter. A gyroscope is usually a sign for complex rotational motion because it rotates in peculiar ways and even seems to defy gravity. These properties make a gyroscope extremely important in everything from a bike to the advanced navigation system on the space shuttle. Certain gyroscopes will only have a single gimbal and therefore have two degrees of freedom (DOF), while a double gimbal gyroscope will have three degrees of freedom overall. A three DOF gyroscope as shown in Figure 1 has been used to carry out the derivation and simulation in this paper.

Autolev™ software is an advanced symbolic manipulator for engineering and mathematical analysis. Its specific purpose is to assist physicists and engineers who use any variant of Newton's law, $\mathbf{F} = m\mathbf{a}$. Autolev™ is capable of using scalars, vectors, dyadics, and matrices to describe the kinematical and dynamical properties of a system. Command lines are input to describe constraints, positions, forces, speeds, accelerations,

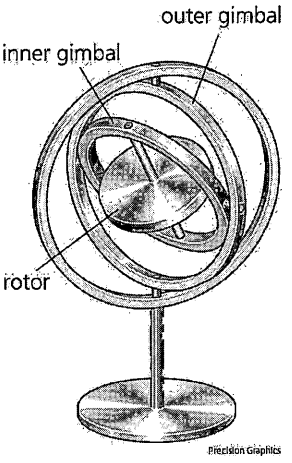


**Figure 1.** Three degree of freedom gyroscope

and other physical properties of each body that will allow the software to make the associated connections between different members within the multi-body system [1].

Multi-body (multi-degree of freedom) dynamical objects, such as the gyroscope in Fig. 1, require many instances of Newton's Law to be "connected" together which causes the motion equations for the last object to become exponentially complex. Essentially all methods following Newton's Law may be used to set up equations of motion for a multi-body system, but some are more suited for computer implementation than others. Among these methods, the Newton-Euler equations, Lagrange's equations, and Kane's equations are three commonly used approaches. The Newton-Euler approach finds a complete solution for all the forces and motion variables involved with a system. Because it treats each body separately, it adds extra computing loads that are associated with the workless constraint forces and these forces are not needed for many applications. The Lagrange's method can automatically eliminate workless constraint forces, but it can be offset by complex derivatives of Lagrangians, which results in a phenomenon of intermediate 'swell' and complex formulation.

Kane's method offers the advantages of both the Newton-Euler and Lagrange methods without the disadvantages. The use of generalized forces eliminates the need to examine any interactive or constraint forces which end up canceling themselves out or are initially zero. Kane's method does not use energy functions so differentiating is not a compounding problem. Kane's method provides an elegant means to develop the dynamics equations for multi-body systems that lends itself to automated numerical computation [2].

## METHODS

To start hand deriving the motion calculations for a three-degree-of-freedom gyroscope, the gyroscope was broken down into the three major components with individual reference frames that represent each piece as shown in the left side of Figure 2. The relative motion of each piece and an assigned variable, $Q_r$ (r=1,2,3), were utilized to make transformation matrices between respective frames. The transformation matrix allows for easy mathematical transformations between reference frames. The position of the D, C, B, or A frame can be expressed in any other frame by using the matrices to calculate direction constants with relatively little effort. The tables in Figure 2 below show the different reference frames with respect to the central mass and gimbals on a gyroscope along with the respective cosine matrices. In Figure 2, Ai>, Bi>, Ci>, and Di> (i=1,2,3) are unit vectors.

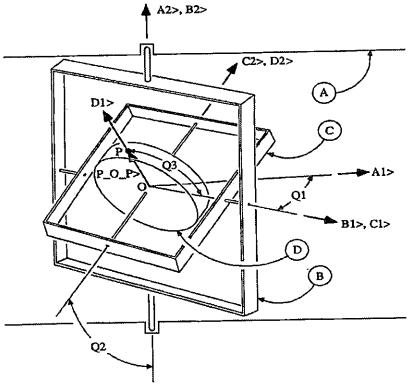


| | $b_1$ | $b_2$ | $b_3$ |
|---|---|---|---|
| $a_1$ | $\cos(q_1)$ | 0 | $-\sin(q_1)$ |
| $a_2$ | 0 | 1 | 0 |
| $a_3$ | $\sin(q_1)$ | 0 | $\cos(q_1)$ |

| | $c_1$ | $c_2$ | $c_3$ |
|---|---|---|---|
| $b_1$ | 1 | 0 | 0 |
| $b_2$ | 0 | $\cos(q_2)$ | $\sin(q_2)$ |
| $b_3$ | 0 | $-\sin(q_2)$ | $\cos(q_2)$ |

| | $d_1$ | $d_2$ | $d_3$ |
|---|---|---|---|
| $c_1$ | $-\cos(q_3)$ | 0 | $-\sin(q_3)$ |
| $c_2$ | 0 | 1 | 0 |
| $c_3$ | $\sin(q_3)$ | 0 | $-\cos(q_3)$ |

**Figure 2.** Gyroscope with reference frames and transformation matrices (A to B, B to C, C to D)

For the motion equations the point P on the gyroscope in Figure 2 will be the point of interest. The velocity of this point was calculated by using point O as a reference for the two points fixed on a rigid body approach shown in Equation 1.1.

$$^{A}\mathbf{v}^{P} = {}^{A}\mathbf{v}^{O} + {}^{A}\boldsymbol{\omega}^{D} \times \mathbf{r}^{OP} \qquad (1.1)$$

where

$^{A}\mathbf{v}^{P}$ is the velocity of point $P$ in the $A$ reference frame,

$^{A}\mathbf{v}^{O}$ is the velocity of point $O$ in the $A$ reference frame,

$^{A}\boldsymbol{\omega}^{D} \times \mathbf{r}^{OP}$ is the cross product of the angular velocity of $D$ with respect to $A$ and the position vector from point $O$ to $P$.

Likewise, the acceleration of point P can be obtained using two points fixed on a rigid body formula as follow

$$^{A}\mathbf{a}^{P} = {}^{O}\mathbf{a}^{P} + {}^{A}\boldsymbol{\omega}^{D} \times ({}^{A}\boldsymbol{\omega}^{D} \times \mathbf{r}^{OP}) + {}^{A}\boldsymbol{\alpha}^{D} \times \mathbf{r}^{OP} \qquad (1.2)$$

where

$^{A}\mathbf{a}^{P}$ is the acceleration of point $P$ in the A reference frame,

$^{O}\mathbf{a}^{P}$ is the velocity of point $P$ with respect to point O,

$^{A}\boldsymbol{\alpha}^{D}$ is the angular acceleration of $D$ with respect to $A$,

$^{A}\boldsymbol{\omega}^{D}$ is the angular velocity of rotor D.

These values are calculated and all transferred into the reference frame A to relate all values for velocity and acceleration into absolute terms.

The general procedure for using Kane's method is to first label important points (important points being defined as all center of mass locations, and locations of applied forces). Secondly, select generalized coordinates, $q_r$ (r=1,2,3), and generalized speeds, $u_r$ (r=1,2,3), and generate the expressions for the angular velocity and acceleration of all bodies and important points. Then by taking partial derivatives of generalized speeds $u_r$ a partial velocity and partial angular velocity table will be produced. For the gyroscope

shown in Figure 2, its kinematical differential equations and angular velocity equations are shown as examples in equations (1.3)-(1.6). Similarly, Table 1 shows its partial angular velocities.

$$\dot{q}_r = u_r \quad (r=1, 2, 3) \tag{1.3}$$

$${}^A\boldsymbol{\omega}^B = -u_1\hat{\mathbf{a}}_2 \tag{1.4}$$

$${}^A\boldsymbol{\omega}^C = -u_2\hat{\mathbf{b}}_1 - u_1\hat{\mathbf{a}}_2 \tag{1.5}$$

$${}^A\boldsymbol{\omega}^D = -u_3\hat{\mathbf{c}}_2 - u_2\hat{\mathbf{b}}_1 - u_1\hat{\mathbf{a}}_2 \tag{1.6}$$

**Table 1.** Partial Angular Velocities

| Generalized Speeds ( $u_r$ ) | ${}^A\boldsymbol{\omega}_r^B$ | ${}^A\boldsymbol{\omega}_r^C$ | ${}^A\boldsymbol{\omega}_r^D$ |
|---|---|---|---|
| r = 1 | $-\hat{\mathbf{a}}_2$ | $-\hat{\mathbf{a}}_2$ | $-\hat{\mathbf{a}}_2$ |
| r = 2 | 0 | $-\hat{\mathbf{b}}_1$ | $-\hat{\mathbf{b}}_1$ |
| r = 3 | 0 | 0 | $-\hat{\mathbf{c}}_2$ |

Kane's Dynamic Equation is then used to obtain the relationship between the generalized active forces involved with the gyroscope and the generalized inertial forces as shown in equation (1.7).

$$F_r + F_r^* = 0 \tag{1.7}$$

where $F_r$ is the rth generalized active force and, $F_r^*$ is the $r^{th}$ generalized inertia force. They are represented in equations (1.8) and (1.9).

$$F_r = \sum_{k=1}^{3}(\boldsymbol{\omega}_r^k \cdot \mathbf{T}^k + \mathbf{v}_r^{\bar{k}} \cdot \mathbf{R}^{\bar{k}}) \qquad (r = 1,2,3;\ k = \text{number of bodies}) \tag{1.8}$$

$$F_r^* = \sum_{k=1}^{3}(\boldsymbol{\omega}_r^k \cdot \mathbf{T}^{k^*} + \mathbf{v}_r^{\bar{k}} \cdot \mathbf{R}^{\bar{k}^*}) \qquad (r = 1,2,3;\ k = \text{number of bodies}) \tag{1.9}$$

In equations (1.8) and (1.9), $\mathbf{v}_r^{\bar{k}}$ is the $r^{th}$ partial velocity of mass center of body $k$, $\mathbf{R}^k$ and $\mathbf{T}^k$ are the resultant force acting on the mass center of body k and the resultant moment acting on body $k$, and $\mathbf{R}^{k^*}$ and $\mathbf{T}^{k^*}$ are the inertia forces and inertial moment acting on body $k$ [3].

## *Results from Autolev™ Codes*

The final velocities and accelerations are expressed within the Autolev™ code to save space because they are quite lengthy but do match the hand calculations exactly. The following command lines set up the gyroscope inside the Autolev™ program and also add in the additional information needed for motion simulation. Command lines 1-4 setup the dimensional aspect of the gyroscope, defining 4 reference frames and defining two points that will be used in the analysis. Lines 5 through 13 are dyadic commands that define the inertial properties that come into effect when either of the two gimbals rotates or when the inner rotor is set in motion. More specifically, command lines 5, 6, 8, and 9

relate the height and width of each gimbal to the inertial forces that would be induced by each specific axis' rotation. Lines 11 and 12 represent the rotation of the rotor about the central radius either in line with the rotating axis or perpendicular to it. The command lines 7, 10, and 13 connect all these terms together into three inertial dyadics which will allow Autolev™ to relate 9 different inertial values into 1 lumped value for the entire system.

```
1. NEWTONIAN A
2. POINT P,O
3. Bodies B,C,D
4. CONSTANTS M{3},H{3},L,W,Y,Z
5. I1=2/3*M1*(H1*W-W^2)
6. I2=1/6*M1*(H1^2)-1/6*M1*(H1-W)^2
7. I_B_BO>>=I1*B1>*B1>+I1*B2>*B2>+I2*B3>*B3>
8. J1=2/3*M2*(H2*W-W^2)
9. J2=1/6*M2*(H2^2)-1/6*M2*(H2-W)^2
10. I_C_CO>>=J1*C1>*C1>+J1*C2>*C2>+J2*C3>*C3>
11. K1=1/2*M3*L^2
12. K2=1/4*M3*L^2+1/12*M3*H3^2
13. I_D_DO>>=K2*D1>*D1>+K1*D2>*D2>+K2*D3>*D3>
```

Lines 14 through 20 create the motion variables that direct the software and simulation data about which reference frame axis the gyroscope will rotate relative to each other. The last five commands in this section give a variable length to the distance from the center of mass (O) to point P and set the velocity and acceleration of point O to zero which is a property of an instantaneous center.

```
14. VARIABLES q{3}',U{3}'
15. SIMPROT(A,B,-2,q1)
16. SIMPROT(B,C,-1,q2)
17. SIMPROT(C,D,-2,q3)
18. Q1'=U1
19. Q2'=U2
20. Q3'=U3
21. P_O_P>=L*D1>
22. V_O_A>=0>
23. A_BO_A>=0>
24. A_CO_A>=0>
25. A_DO_A>=0>
```

Results from lines 28 and 30 display the absolute velocities and accelerations of point P in the A reference frame. Both terms are long and bulky but are consistent with the data derived by hand earlier.

```
26. V2PTS(A,D,O,P)
27. EXPRESS(V_P_A>,A)
```

```
28. EXPAND(V_P_A>)
29. A_O_A>=0>
30. A_P_A>=EXPRESS(A_P_A>,A)
31. MASS B=M1, C=M2, D=M3
32. TORQUE_B>=Y*A2>
33. TORQUE_C>=Z*B1>
```

Lines 31 through 33 express different variables that were used for the motion simulation representing different masses of pieces and the distinct torques on each gimbal. Below are the commands to invoke the software to calculate the generalized active and inertial forces used in Kane's Method.

```
34. ZERO=FR() + FRSTAR()
35. KANE()
```

Finally the last nine lines of code direct the program to label certain values that will be input into the multi-body system for motion simulation and what type of code Autolev™ writes.

```
36. UNITS M1=KG,M2=KG,M3=KG,T=SEC,H1=m,H2=m,H3=m
37. UNITS L=m,W=m,Y=N*m,Z=N*m
38. UNITS Q1=DEG,Q2=DEG,Q3=DEG,U1=RAD/SEC,U2=RAD/SEC,U3=RAD/SEC
39. INPUT L=.3,W=.025,H1=.6,H2=.5,H3=.4
40. INPUT M1=2,M2=2,M3=50,Y=0,Z=10
41. INPUT Q1=0,Q2=0,Q3=0,U1=0,U2=0,U3=10
42. INPUT TFINAL=5,INTEGSTP=.05,ABSERR=1.0E-07,RELERR=1.0E-07
43. OUTPUT T,Q1,Q2,Q3,U1,U2,U3
44. CODE DYNAMICS() PHASE3.M,SUBS
```

The previous code was compiled by Matlab™ and the resultant output file was graphed to show the angular motion of the gyroscope under three different input conditions. Figure 3 shows the data for Trial 1, Figure 4 for Trail 2, and Figure 5 for Trail 3. The left graph shows the angles that the outer gimbal, inner gimbal, and rotor passed through while the right graph shows the acceleration of point P during the simulation. For the left graph the lower line represents the angle Q1 (outer gimbal), middle line shows Q2 (inner gimbal), and upper line is the data for Q3 (rotor). The right graph represents the resultant acceleration of point P during the trial period.

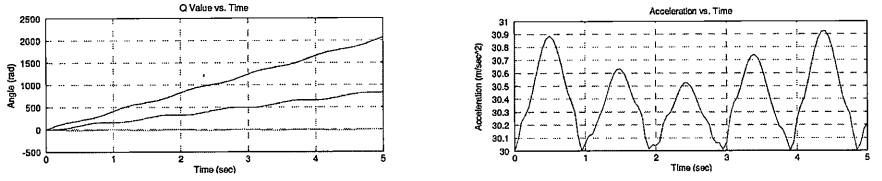


**Figure 3.** Trial 1 – Rotor Spinning at 10 rad/sec. Torque on B is 10 N/m.

During Trial 1 the internal rotor was initially spinning at 10 rad/sec and all torques on reference frames were equal to zero except for a 10 N/m force on frame B set in the positive direction. The rate of change in angle of Q3 (Frame D), the rotor, is about twice as fast as Q1 (Frame B), while Q2 (Frame C) does not even rotate all the way around, but has a slight rocking effect which was unexpected. The point P has a fairly steady acceleration cycle with a constant period where the amplitude, however, does change slightly which is probably due to the slight unexpected rocking of the C reference frame.

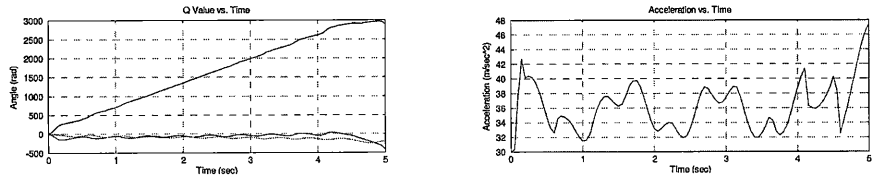


**Figure 4.** Trial 2 – Rotor Spinning at 10 rad/sec. Torque on B and C is 10 N/m.

For the second trial the conditions were altered by adding a second torque to the system on reference frame C with a magnitude of positive 10 N/m while retaining the other initial conditions of Trial 1. The rotor, Q3 (D), in Trial 2 controls most of the motion in the gyroscope leaving Q1 (B) and Q2 (C), which are the inner and outer gimbals, at about the same angular position as where they started. Because the 10 N/m force was not great enough to completely spin either the B or C frame a rocking motion is created inside both frames. The acceleration data is almost the same as the first trial but has small fluctuations within the waveform. The rocking of both frames B and C caused by the addition of a torque force on the C reference frame created the deflections in the acceleration graph on the right.

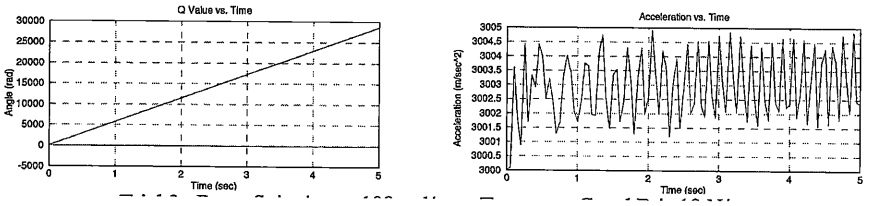


**Figure 5.** Trial 3 – Rotor Spinning at 100 rad/sec. Torque on C and D is 10 N/m.

The third trial has the same conditions as Trial 2 but the rotor's speed has been increased by 10 times to 100 rad/sec. The movement of the rotor, Q3 dominates all motion in gyroscope leaving Q1 (B) and Q2 (C) at the same angular position compared to magnitude of Q3 (D). The magnitude of the acceleration of point P has increased approximately 100 times that of the previous trials which is expected since the acceleration varies as the square of the angular velocity. There are very small fluctuations within the acceleration graph that point out a small rocking effect remains in the system even though it cannot be seen on the left graph.

# DISCUSSION

Many methods can be used to analyze and create motion equations for complex multi-body systems. The method utilized within this paper, Kane's method, can be seen as the most efficient mode to create these equations with the most time savings, least complications, and smallest amount of unnecessary calculations. By using the Autolev™ program a three-degree-of-freedom system can be solved by utilizing only 44 main commands. There are 16 different variables within the program and only 3 were manipulated for this project, one speed and two torque values. Virtually any situation can be created and analyzed with this program in a matter of minutes versus hours and days when analyzing each individual situation by hand. The motion of each aspect of the gyroscope in each of the three different trials had expected results as well as a few unexpected situations. The major motion of the gyroscope was expected, but there was some minor rocking within the system that caused small fluctuations in the acceleration of the selected point P. By using Kane's method the workload for the hand derivation was cut to a minimum, only calculating the needed values while keeping the equations at a controllable size. Kane's method is still a relatively new technique for solving multi-body systems but as technology has evolved so have the methods used to utilize and create this technology. Kane's method is an effective means for solving multi-body systems in a proficient manner and will be seen more and more as technology advances.The three-degree-of-freedom problem in this paper is just the tip of what Kane's method is capable of; the motion properties of the inner gimbal, outer gimbal, and rotor have relatively small and simple equations when compared to the motion equations used to control a space shuttle or robotic being.

## REFERENCES

[1] www.autolev.com—Autolev Webpage
[2] Huston, Ronald L. *Multi-body Dynamics*. Boston: Butterworth-Heinemann, 1990.
[3] Kane, T. R. and Levision, D. A. Dynamics Online: Theory and Implementation with Autolev. Online Dynamics, Inc. 2000.